

Rehabilitation of a stiffened arch bridge

Autor(en): **Honda, Hideyuki / Kido, Takayoshi / Kobori, Tameo**

Objekttyp: **Article**

Zeitschrift: **IABSE proceedings = Mémoires AIPC = IVBH Abhandlungen**

Band (Jahr): **10 (1986)**

Heft P-96: **Rehabilitation of a stiffened arch bridge**

PDF erstellt am: **28.06.2024**

Persistenter Link: <https://doi.org/10.5169/seals-39605>

Nutzungsbedingungen

Die ETH-Bibliothek ist Anbieterin der digitalisierten Zeitschriften. Sie besitzt keine Urheberrechte an den Inhalten der Zeitschriften. Die Rechte liegen in der Regel bei den Herausgebern.

Die auf der Plattform e-periodica veröffentlichten Dokumente stehen für nicht-kommerzielle Zwecke in Lehre und Forschung sowie für die private Nutzung frei zur Verfügung. Einzelne Dateien oder Ausdrucke aus diesem Angebot können zusammen mit diesen Nutzungsbedingungen und den korrekten Herkunftsbezeichnungen weitergegeben werden.

Das Veröffentlichen von Bildern in Print- und Online-Publikationen ist nur mit vorheriger Genehmigung der Rechteinhaber erlaubt. Die systematische Speicherung von Teilen des elektronischen Angebots auf anderen Servern bedarf ebenfalls des schriftlichen Einverständnisses der Rechteinhaber.

Haftungsausschluss

Alle Angaben erfolgen ohne Gewähr für Vollständigkeit oder Richtigkeit. Es wird keine Haftung übernommen für Schäden durch die Verwendung von Informationen aus diesem Online-Angebot oder durch das Fehlen von Informationen. Dies gilt auch für Inhalte Dritter, die über dieses Angebot zugänglich sind.

Rehabilitation of a Stiffened Arch Bridge

Remise en état d'un pont arc

Sanierung einer versteiften Bogenbrücke

Hideyuki HONDA

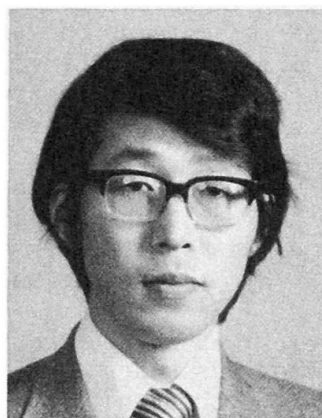
Assoc. Prof.
Kanazawa Inst. of Technol.
Kanazawa, Japan



Hideyuki Honda, born 1950, obtained the degree of Doctor of Engineering at Kyoto Univ. He is researching the dynamic effects of highway bridges under moving vehicles.

Takayoshi KIDO

Assistant
Kanazawa University
Kanazawa, Japan



Takayoshi Kido, born 1952, has been working at Kanazawa University since 1970. He is researching the repair and the rehabilitation of highway bridges.

Tameo KOBORI

Prof. Dr.
Kanazawa University
Kanazawa, Japan



Tameo Kobori, born 1930, obtained the degree of Doctor of Engineering at Kyoto Univ. Since 1971, he has been a professor of structural engineering at Kanazawa University.

SUMMARY

An analytical and experimental study of the rehabilitation of a stiffened arch bridge is presented. In order to determine the most efficient method of reinforcement for this bridge, the statistical inference method was applied. Based on an analytical study, diagonal members were added to the structure. Both the analytical study and a field test showed the rehabilitation of this bridge by reinforcement with diagonal members to be successful.

RÉSUMÉ

Une étude analytique et expérimentale de la remise en état d'un pont arc avec sous-tirant est présentée. Afin de déterminer la méthode de renforcement la plus adéquate pour ce pont, la méthode statistique des inférences a été utilisée. Suite à une étude analytique, la structure a été renforcée à l'aide de barres diagonales. Aussi bien l'étude analytique que les essais ont montré le bien-fondé de ce type de renforcement.

ZUSAMMENFASSUNG

Theoretische und experimentelle Untersuchungen einer versteiften Bogenbrücke werden vorgestellt. Um die wirkungsvollste Art der Verstärkung der Brücke zu bestimmen, wurde die Methode der statistischen Analyse angewandt. Basierend auf den theoretischen Überlegungen wurden Diagonalstäbe angebracht. Sowohl die theoretischen Untersuchungen als auch die Messungen haben dann gezeigt, dass die Sanierung mit Diagonalstäben erfolgreich war.



1. INTRODUCTION

A variety of technical problems related to highway bridges have arisen in recent years due to the increasing number of heavy trucks on highways, and the method of reinforcement of bridges has become a subject of wide interest. In the reinforcement of bridges it is necessary to consider not only static and dynamic problems, but also the serviceability based on vibration felt by pedestrians [2]. It is therefore necessary to determine the configuration of reinforcement chords which most effectively solves these problems.

In this paper a particular stiffened arch bridge (Lohse girder bridge), which exhibited the problems described above, is considered as a case study. Reinforcement by the addition of diagonal members was investigated. In order to determine the most efficient and economical method of reinforcement for this bridge, a statistical inference method used in the design of experiments [5] was applied to this study. In this method the rehabilitation of the bridge was evaluated in terms of two values: the acceleration corresponding to the dynamic behaviour of the bridge, and the velocity corresponding to the vibration felt by a pedestrian. Each effective value of the response acceleration and velocity was calculated by dynamic analysis of nonstationary response of the bridge under a moving heavy vehicle, and the optimum combination of diagonal members was estimated by the statistical inference method using these effective values. The effect of the addition of the estimated optimum combination of diagonal members on the static and dynamic behaviour and the vibration felt by pedestrians was investigated.

Using the calculated results described above, and taking aesthetic points into consideration, actual construction was undertaken to reinforce the bridge. The bridge was tested before and after construction to investigate the effect of addition of the diagonal members. From the results of the analytical study and the field test it can be seen that there is confirmation of the predictions of the analytical study, showing that the method of reinforcement using diagonal members was successful for the rehabilitation of stiffened arch bridge.

2. ANALYTICAL STUDY

2.1 Statistical procedure

The considered bridge is illustrated in Fig.1 and Photo.1. This bridge was designed according to the highway bridge specification(1939) with a vehicle load of 127.4 kN, and was constructed in 1955. In recent years an increasing number of heavy trucks, which far exceed the design vehicle load for this bridge, has been experienced, and the concrete in the RC slab had partially deteriorated. When the load carrying capacity of this bridge based on the current design specification was calculated, the strength of the RC slab and the stiffening girder were found to be insufficient. In a former vibration test on this bridge, it had been recognized that a high first asymmetric vibration was caused by its resonating at the natural frequency of heavy moving vehicles, and many pedestrians had difficulty walking because of this vibration. To solve these technical problems two effective values of acceleration and velocity of vibration were adopted to improve the dynamic characteristics of the bridge under a moving vehicle. The acceleration corresponds to the magnitude of bridge vibration, while the velocity corresponds to the vibration felt by a pedestrian.

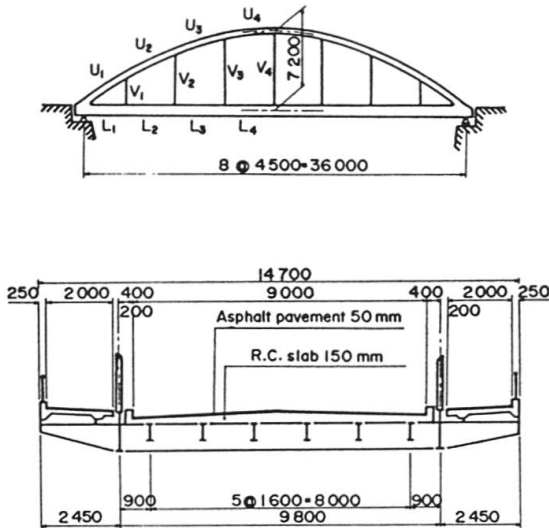


Fig.1 Details of considered bridge.

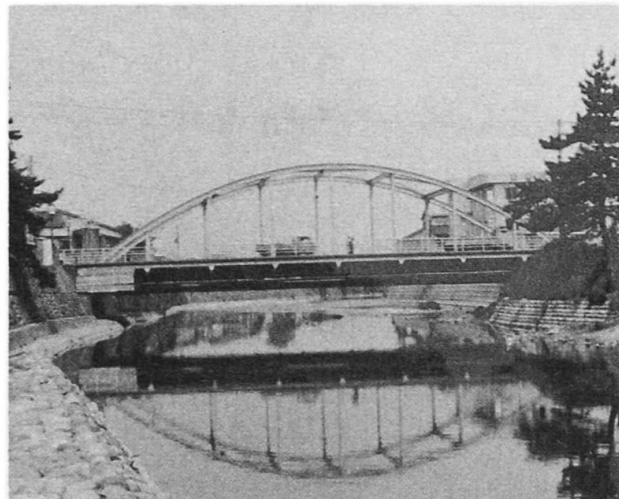


Photo.1 View of NAKAJIMA bridge (constructed 1955).

In order to reduce these effective values, an alteration of the structural system of this bridge was considered. The addition of diagonal members to this bridge was evaluated by tests on a 1/10 scale model of the bridge. It was confirmed that the damping capacity of this model bridge with the diagonal members was increased. Fig.2 shows the positions from A to F of diagonal members which may influence effective values of the response acceleration and velocity. These diagonal hangers are considered as a factor in the statistical inference method, and each factor has 2 levels as "added" or "not added" to this bridge [5].

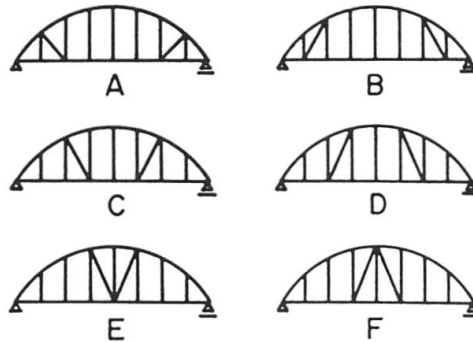


Fig.2 Position of diagonal members (factors).

The fixed-effect model of these effective values is defined as,

$$Y = f(x_{A_i}, x_{B_j}, x_{C_k}, x_{D_l}, x_{E_m}, x_{F_n}) = X\mu + \epsilon \quad (1)$$

in which Y = Effective vector; x_{A_i} = value of the factor x_A at the level i ; X = Design matrix of factor; μ = Unknown parameter vector; $X\mu$ = Treatment-population mean on combination of each factor; ϵ = Error vector.

In the design matrix an orthogonal array plan arranged with each factor in a orthogonal array table was adopted. This plan can facilitate the analysis of the fixed-effect model, because the arranged factors do not interact in the orthogonal array. Each factor from A to F is arranged in an orthogonal array table OA(32,31,2,2) [6], and is allocated to each column of 1,2,4,8,16 and 31 in OA(32,31,2,2), respectively. Although there are 64 (2^6) combinations of the six diagonal members, this allocation has thirty-two combinations for a one-half factorial design. Eq.(1) is rewritten so that the allocation of factors is:



$$\begin{aligned}
 Y &= x_1^{\mu_1} + x_A^{\mu_A} + x_B^{\mu_B} + x_{AB}^{\mu_{AB}} + x_C^{\mu_C} \\
 &+ x_{AC}^{\mu_{AC}} + x_{BC}^{\mu_{BC}} + x_{ABC}^{\mu_{ABC}} \\
 &+ x_D^{\mu_D} + \dots + x_{EF}^{\mu_{EF}} + x_E^{\mu_E} \\
 &+ x_{AE}^{\mu_{AE}} + \dots + x_{AF}^{\mu_{AF}} + x_F^{\mu_F} + \varepsilon
 \end{aligned} \quad (2)$$

in which $x_1^{\mu_1}$ = the generalized mean, the subscript AB of $x_{AB}^{\mu_{AB}}$ = the combination of factors A and B , each term from $x_A^{\mu_A}$ to $x_F^{\mu_F}$ is the treatment-effect defined as the difference from $x_1^{\mu_1}$.

2.2 Calculation of effective values

Fig.3 shows the vehicle-bridge vibration system. The deflection of the bridge in Fig.3 as given by modal analysis is:

$$y(t, x) = \sum_{n=1}^{\infty} q_n(t) \phi_n(x) \quad (3)$$

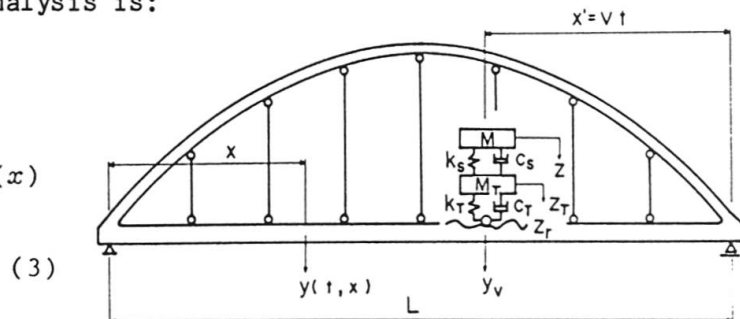


Fig.3 Vehicle-bridge system.

in which $y(t, x)$ = Deflection of bridge; $q_n(t)$ = Generalized coordinate; $\phi_n(x)$ = Vibration mode function; t = Time counted from the moment when the moving vehicle comes to the bridge; x = Coordinate in right direction of bridge with origin at left side support of bridge.

The mode function $\phi_n(x)$ is defined by the series:

$$\phi_n(x) = \sum_{m=1}^{\infty} a_{nm} \sin \frac{m\pi x}{L} \quad (4) \quad \sum_{m=1}^{\infty} a_{nm}^2 = \frac{2}{\rho L} \quad (5)$$

in which, using the span length L and the bridge mass ρ per unit span length, the parameter a_{nm} is normalized by the function of Eq.(5). The equation of motion on the vehicle-bridge system is obtained by an energy method as

$$\ddot{q}_n(t) + 2h_n \omega_n \dot{q}_n(t) + \omega_n^2 q_n(t) = -(M\ddot{z} + M_T\ddot{z}_T)\phi_n(Vt) \quad (6)$$

in which h_n = Damping constant of bridge; ω_n = n -th natural circular frequency of bridge; M = Sprung mass of vehicle; M_T = Unsprung mass of vehicle; k_S = Suspension-spring stiffness of vehicle; k_T = Tire-spring stiffness of vehicle; c_S = Suspension-damping factor of vehicle; c_T = Tire-damping factor of vehicle; z_r = Road surface roughness;

\ddot{z} = Vertical acceleration of sprung mass; \ddot{z}_T = Vertical acceleration of unsprung mass; V = Velocity of vehicle.

When the vehicle moves across a bridge with random-road surface roughness, the right side in Eq.(6) is the stationary-external force $f(t)$ toward the bridge. If $\phi_n(Vt)$ is considered as the deterministic function in the nonstationary process produced by movement of the vehicle, Eq.(6) reduces to a linear response problem with one degree of freedom under the nonstationary-external force [4]. Therefore, the mean square value is calculated as the average quantity of the response vibration produced only when a vehicle is moving on the bridge. Using the power spectral density (PSD), $S_f(\omega)$, of the stationary-external force $f(t)$, the mean square value of the response velocity and of the acceleration at each point of calculation x is then obtained as:

$$E [\dot{y}^2(t, x)] = \sum_{n=1}^{\infty} \{ E [\dot{q}_n^2(t)] \phi_n^2(x) \} \quad (7)$$

$$E [\ddot{y}^2(t, x)] = \sum_{n=1}^{\infty} \{ E [\ddot{q}_n^2(t)] \phi_n^2(x) \} \quad (8)$$

where,

$$\begin{aligned}
 E [\dot{q}_n^2(t)] &= \frac{2 \exp(-2h_n \omega_n t)}{\bar{\omega}_n^2} \int_0^{\infty} S_f(\omega) \\
 &\times \left[\left\{ -h_n \omega_n I_S(\omega, t) + \frac{\partial I_S(\omega, t)}{\partial t} \right\}^2 \right. \\
 &\left. + \left\{ -h_n \omega_n I_C(\omega, t) + \frac{\partial I_C(\omega, t)}{\partial t} \right\}^2 \right] d\omega \quad (9)
 \end{aligned}$$

$$\begin{aligned}
 E [\ddot{q}_n^2(t)] &= \frac{2 \exp(-2h_n \omega_n t)}{\bar{\omega}_n^2} \int_0^{\infty} S_f(\omega) \\
 &\times \left[\left\{ (h_n \omega_n)^2 I_S(\omega, t) - 2h_n \omega_n \frac{\partial I_S(\omega, t)}{\partial t} + \frac{\partial^2 I_S(\omega, t)}{\partial t^2} \right\}^2 \right. \\
 &\left. + \left\{ (h_n \omega_n)^2 I_C(\omega, t) - 2h_n \omega_n \frac{\partial I_C(\omega, t)}{\partial t} + \frac{\partial^2 I_C(\omega, t)}{\partial t^2} \right\}^2 \right] d\omega \quad (10)
 \end{aligned}$$

in which $\bar{\omega}_n = \omega_n \sqrt{1-h_n}$. The details of $I_S(\omega, t)$, $I_C(\omega, t)$, $\partial I_S(\omega, t)/\partial t$, $\partial I_C(\omega, t)/\partial t$, $\partial^2 I_S(\omega, t)/\partial t^2$ and $\partial^2 I_C(\omega, t)/\partial t^2$ in Eqs. (9) and (10) are shown in reference [4]. The maximum value of the root mean square (r.m.s.) to the response acceleration is adopted as the effective value of the magnitude of the bridge vibration. The average value $\bar{\sigma}_v$ of the r.m.s. of response velocity is adopted as the other effective value of the psychological effect on the pedestrian, and it is defined as,

$$\bar{\sigma}_v = \left\{ \frac{1}{T} \int_0^T E [\dot{y}^2(t, x)] dt \right\}^{1/2} \quad (11)$$

in which $T = L/V$, and Eq.(11) indicates the average vibration felt by a pedestrian only when the vehicle is moving on the bridge.



The characteristic of road surface roughness is expressed generally by the PSD, which is assumed from a stationary normal probability process with a zero mean value. It has been previously shown by the authors that the PSD for road surface roughness can be approximated by an exponential function [1]. In this study the road surface roughness of the investigated bridge was measured by surveyor's level at 10 cm intervals, 0.5 m from the center line of the road. The PSD of the road surface based on the measured roughness data was calculated by a maximum entropy method (MEM) and approximated by an exponential function as illustrated in Fig.4. The properties of the vehicle load and the road surface are shown in Table 1.

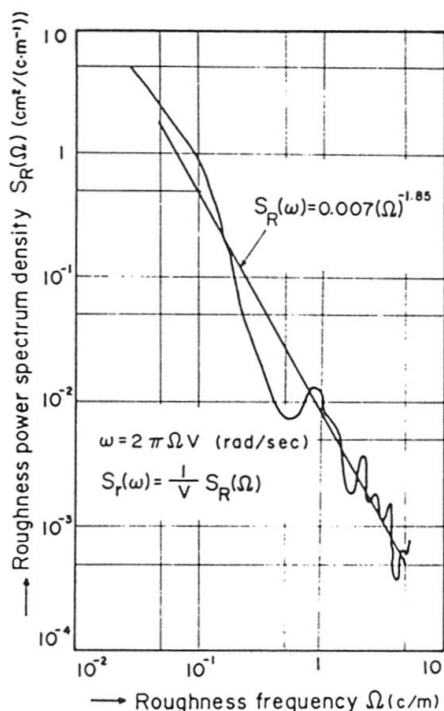


Fig.4 PSD of road surface roughness.

Table 1 Vehicle load and roadway properties.

Velocity (V): 10 m/sec	
Wavelength of roadway roughness: 20cm - 20 m	
PSD of roadway roughness ($\text{cm}^2 \cdot \text{sec}/\text{c}$): $S_p(\omega) = 0.007V^{0.85}(\omega/2\pi)^{1.85}$	
Vehicle weight: 196kN (Upper;176.4kN, Lower;19.6kN)	
Spring stiffness	k_s : 3920kN/m - 5880kN/m k_t : 7840kN/m - 11760kN/m
Damping factor	c_s : 24.5kN/m/s, c_t : 29.4kN/m/s
PSD of vehicle load (White noise with bandwidth ω)	$3\pi - 7\pi$ rad/sec (1.5 - 3.5Hz): $S_f(\omega) = 17.938 \text{ kN}^2 \cdot \text{s}$
	$20\pi - 40\pi$ rad/sec (10 - 20 Hz): $S_f(\omega) = 3.051 \text{ kN}^2 \cdot \text{s}$

The PSD of external force on the vehicle load is expressed by two bands of white noise with bandwidth ω , because heavy vehicles having properties of various frequencies must be also considered. The strength of this white noise was determined by the mean power (variance) of the PSD on the vehicle load. The damping constant h_n of the bridge was assigned the value of 0.017. Each diagonal member added to the bridge has a section of H-118 x 249 x 8 x 8.

According to the method of treatment of the diagonal members, each effective value of the response acceleration and velocity was calculated by Eqs.(8) and (11) using dynamic analysis of nonstationary response of the bridge with the added diagonal members under a moving heavy vehicle. These calculated results are illustrated in Table 2. In this Table, when each diagonal member is not added to the bridge, the value of 0 is taken, and when each one is added, the value of 1 is taken. The dynamic characteristics of the bridge differ with each combination of diagonal members. For Nos. 1, 10 and 25, the first natural frequency of the bridge corresponds to asymmetric vibration, while all other combinations produce symmetric vibration.

Table 2 Natural frequencies and effective values for various conditions.

No.	Case treated						Natural frequency (Hz)		Response acceleration (cm/sec ²)	Response velocity (cm/sec)
	A	B	C	D	E	F	1st	2nd		
1	0	0	0	0	0	0	3.06	4.12	48.77	2.163
2	0	0	0	0	1	1	3.12	6.23	21.66	0.637
3	0	0	0	1	0	1	3.73	6.86	20.38	0.616
4	0	0	0	1	1	0	3.79	7.03	19.21	0.585
5	0	0	1	0	0	1	3.84	6.87	19.32	0.584
6	0	0	1	0	1	0	3.86	6.31	18.61	0.567
7	0	0	1	1	0	0	3.84	4.62	22.78	0.666
8	0	0	1	1	1	1	3.85	8.06	18.34	0.564
9	0	1	0	0	0	1	3.73	5.80	22.60	0.657
10	0	1	0	0	0	0	3.18	4.22	46.05	1.982
11	0	1	0	1	0	0	3.79	4.50	21.60	0.706
12	0	1	0	1	1	1	3.84	7.82	19.21	0.584
13	0	1	1	0	0	0	3.89	4.55	23.04	0.758
14	0	1	1	0	1	1	3.90	7.42	18.53	0.563
15	0	1	1	1	0	1	3.88	7.31	18.83	0.572
16	0	1	1	1	1	0	3.89	7.23	18.14	0.556
17	1	0	0	0	0	1	3.87	6.00	21.32	0.625
18	1	0	0	0	1	0	3.93	5.47	19.67	0.587
19	1	0	0	1	0	0	3.88	4.43	22.66	0.710
20	1	0	0	1	1	0	3.93	7.86	18.94	0.572
21	1	0	1	0	0	0	3.94	4.44	23.18	0.760
22	1	0	1	0	1	1	3.97	7.44	18.33	0.556
23	1	0	1	1	0	1	3.94	7.30	18.77	0.569
24	1	0	1	1	1	0	3.95	7.23	18.06	0.552
25	1	1	0	0	0	0	3.39	4.41	39.40	1.609
26	1	1	0	0	1	1	3.95	6.61	19.86	0.588
27	1	1	0	1	0	1	3.90	6.92	19.97	0.588
28	1	1	0	1	1	0	3.95	7.04	18.73	0.567
29	1	1	1	0	0	1	3.97	6.93	18.62	0.564
30	1	1	1	0	1	0	3.98	6.36	17.87	0.547
31	1	1	1	1	0	0	3.96	4.51	22.94	0.667
32	1	1	1	1	1	1	3.98	8.05	18.16	0.552

2.3 Statistical inference

When the estimator of μ in Eq.(1) is given by $\hat{\mu}$, the estimator $\hat{\mu}$ is obtained by the least squares method as,

$$\hat{\mu} = (X^t X)^{-1} X^t Y \tag{12}$$

Each sum of squares which is indicated by the component of each fixed-factorial effect is written with this estimator $\hat{\mu}$ as,

$$\begin{aligned} Y Y^t &= \hat{\mu}_1 X_1^t Y + \hat{\mu}_A x_A^t Y + \hat{\mu}_B x_B^t Y + \hat{\mu}_{AB} x_{AB}^t Y \\ &+ \hat{\mu}_C x_C^t Y + \hat{\mu}_{AC} x_{AC}^t Y + \dots + \hat{\mu}_{ABC} x_{ABC}^t Y \\ &+ \hat{\mu}_D x_D^t Y + \dots + \hat{\mu}_{AF} x_{AF}^t Y + \hat{\mu}_F x_F^t Y \end{aligned} \tag{13}$$

Using the estimator of error $\hat{\mu}_0 x_0^t Y$, the F^* value in an analysis of variance is defined by,

$$F^* = (\hat{\mu} x^t Y / \phi) / (\hat{\mu}_0 x_0^t Y / \phi_0) \tag{14}$$

in which ϕ and ϕ_0 is the degree of freedom "not neglected" and "neglected" in these sums of squares. In F-test, if this F^* is greater than the value of F-Table $F(\phi, \phi_0, \alpha)$ to the level of significance α , then each



fixed-factorial effect of these factors is recognized. The calculated results based on analysis of variance as described above is illustrated in Table 3.

Table 3 Results of analysis of variance.

Effective values	Factorial effects
Acceleration	$C^{**}, D^*, E^{**}, F^{**}, C*D^{**}, E*F^{**}$
Velocity	$C^{**}, D^{**}, E^{**}, F^{**}, E*F^{**}$

*: Level of significance 5%

** : Level of significance 1%

C: Main effect of factor C

$C*D$: Interaction effect of factor C and D

It was found that these main effects of factors C, D, E and F, and the interaction effect $E*F$ of factors E and F interact with each effective value, but the factors A and B do not interact. Hence, using these significant factors, the optimum combination of these diagonal members was estimated by the Yates's method for the population mean and is illustrated in Fig.5.

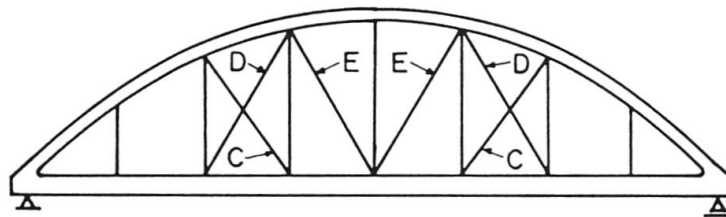


Fig.5 Optimum combination of diagonal members (C, D and E).

The optimum combination shown in this Figure results from the fact that the combination of diagonal members C, D and E has greater shearing stiffness than that of the other members A, B and F.

2.4 Effect of optimum combination

The effect of addition of the estimated optimum combination on the vibration felt by the pedestrian, and on the static and dynamic problems was investigated. As a numerical example, Figs.6 (a)-(e) show the influence line of bending moment, deflection, shearing force, axial force and the composite stress of bending moment and axial force, respectively, on the stiffening girder. Figs.7 (a) and (b) show the influence line of bending moment and the composite stress on the arch member. The solid line and the dotted line in these figures show the structure systems with and without the addition of the C, D and E combination of diagonal members. Comparing the solid line with the dotted line at point $L/4$, it can be seen that the influence line of bending moment on the stiffening girder decreases to $1/3$ (Fig.6(a)). In the arch member, it decreases to $1/5$ (Fig.7(a)). In addition, the influence lines of deflection on the stiffening girder and the arch member decrease about $1/2 - 1/4$ (Fig.6(b)), although this is not shown in Fig.7. Although the shearing force shown by the dotted line is less than the solid line, as shown in Fig.6(c), the axial force shown by the dotted line is slightly greater than the solid line, as shown in Fig.6(d). When the influence lines of composite stress of bending moment and axial force on the stiffening girder and arch member were calculated as shown in Fig.6(e) and Fig.7(b), it became clear

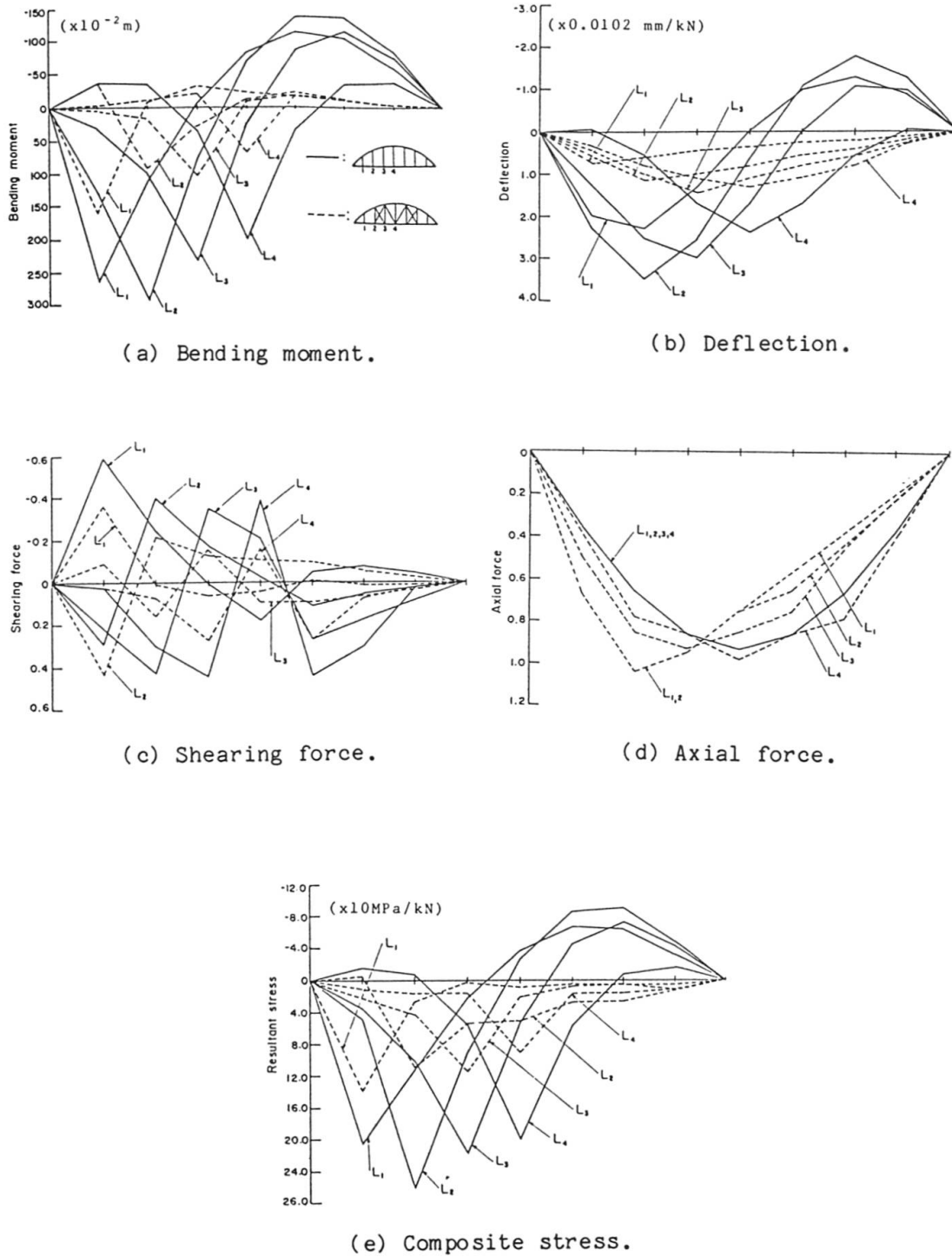


Fig.6 Each influence line of stiffening girder.

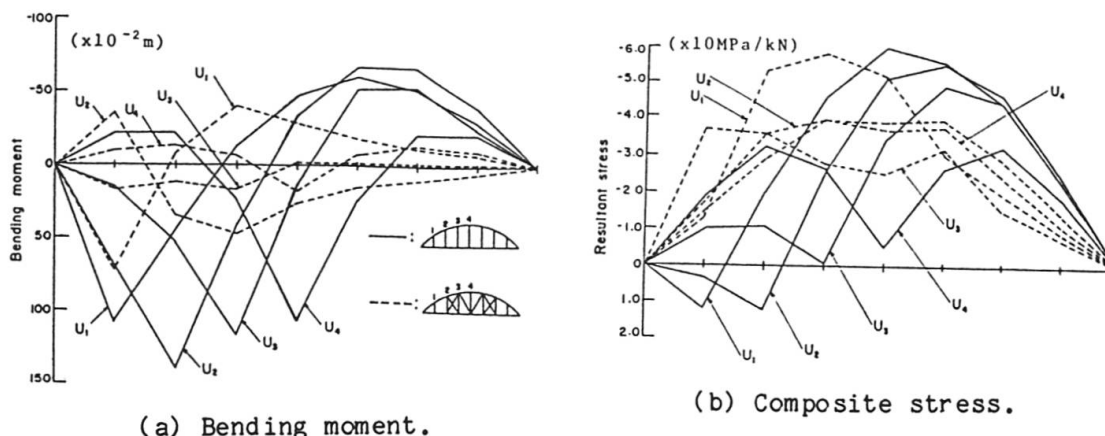


Fig.7 Each influence line of arch member.

that addition of the C , D and E combination of the diagonal members reduces the stress. However, it is necessary to make sure that the increase in axial force on the arch member caused by the diagonal members does not cause buckling.

In static problems, the bridge with the added diagonal members C , D and E , has the characteristics of a Nielsen system stiffening arch bridge [7]. In addition, the load carrying capacity of the bridge increases because the applied load is dispersed by these diagonal members. Thus, when a stiffening girder as in the case of the considered bridge has not enough load carrying capacity, the method of reinforcement using diagonal members is a successful way to improve the static characteristics of the stiffened arch bridge.

In dynamic problems, when the natural frequency of the stiffened arch bridge was calculated, a value of 3.06 Hz was obtained for the first asymmetric mode, and 4.12 Hz for the symmetric mode. It can be considered that this value of 3.06 Hz may be resonant with the natural frequency of heavy vehicles, resulting in the large first asymmetric vibration. However, when the bridge was reinforced by the optimum combination C , D and E , the asymmetric frequency increased to 7.20 Hz, and the symmetric frequency conversely decreased to 3.85 Hz. When only the first frequency was considered, it was found that the frequency increased from 3.06 Hz to 3.85 Hz, and in addition, the vibration mode was changed by the alteration of the bridge structure system from an asymmetric mode to a symmetric one.

Fig.8 shows the relationship between the bridge structure systems and the effective values. The solid line and the dotted line show the calculated results of dynamic response based on Eqs.(7) and (8) at the points of calculation $L/4$ and $L/2$ of the span. In comparing the solid line with the dotted line, the maximum value of r.m.s. to the response acceleration decreases by about $1/2.7$. Finally, the bridge when reinforced by the optimum combination of diagonal members has the same characteristics as a Nielsen system stiffening arch bridge [7], and so the large first asymmetric vibration can be eliminated, achieving one of the goals of this study.

The vibration felt by a pedestrian is evaluated from the r.m.s. value of response velocity shown in Fig.8. By comparing the solid line and the dotted line, it can be seen that the maximum value of this r.m.s. decreases by about $1/3$ when the bridge is reinforced by the optimum combination of diagonal members: a rather pronounced effect.

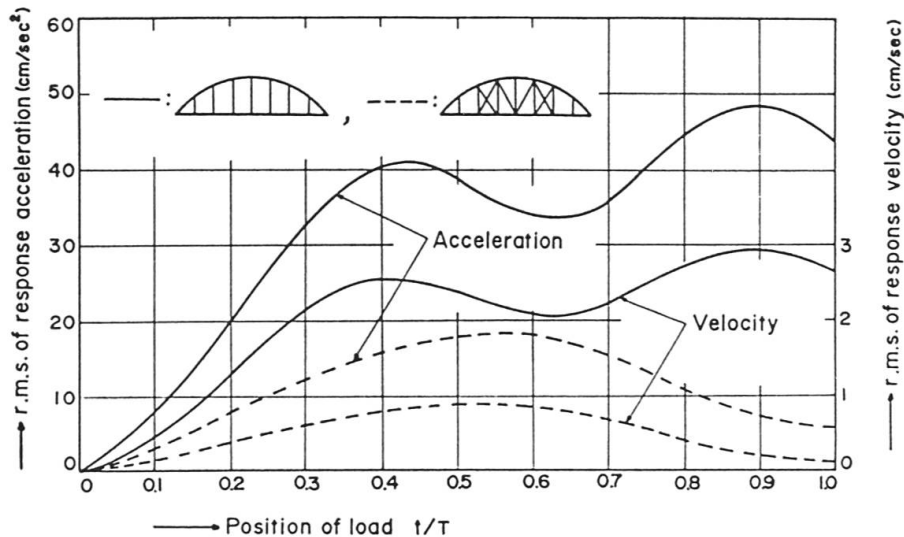


Fig.8 Relation between structural systems and effective values.

In addition, when the average value of this r.m.s. was calculated by Eq.(11), the result was 2.163 cm/s for the stiffened arch bridge and 0.561 cm/s for the reinforced bridge. From reference {3}, this value of 2.163 cm/s corresponds to these subjective responses: 90% of pedestrians clearly feel the vibration and 40% experience difficulty walking. On the other hand, at 0.561 cm/s: 50% of pedestrians feel a small vibration, although less than 10 % of those feel it clearly. Therefore, the serviceability in terms of vibration felt by pedestrians is clearly improved when the bridge is reinforced by the optimum combination of diagonal members.

3. EXPERIMENTAL STUDY

From the calculated results based on the analytical study described above, it was found that the method of reinforcement by the optimum combination of diagonal members was successful for this bridge. However, the aesthetic factor was an important consideration because this bridge was in the city. Therefore, in the actual construction, it was not desirable to apply these calculated results for the reinforcement of this bridge. Instead, using the effectiveness of the diagonal members calculated in the analytical study, and taking aesthetics into consideration, the actual reinforcement chosen involved diagonal members combined as a Warren type as shown in Photo.2. The chord of H - 118 x 249 x 8 x 8 was adopted as the section of each



Photo.2 Reinforced bridge.

study, and taking aesthetics into consideration, the actual reinforcement chosen involved diagonal members combined as a Warren type as shown in Photo.2. The chord of H - 118 x 249 x 8 x 8 was adopted as the section of each



diagonal member. Therefore, although it was impossible to verify exactly the calculated results because the actual combination of the diagonal members differed from the optimum combination, testing before and after construction was carried out to determine the effect of reinforcement by addition of such diagonal members.

To increase the load carrying capacity of the stiffening girder, the lower flange was welded by channel steel in situ, and the section of this flange was reinforced.

Table 4 Load carrying capacity.

Item	Reinforcement							
	Not applied				Applied			
	σ_a	σ_d	σ_l	P	σ_a	σ_d	σ_l	P
Slab	50*	6	64	13.8	80*	2	63	24.7
Stringer	1400	251	1204	19.0	1400	217	846	28.0
End floor beam	1400	266	1709	13.2	1400	316	832	26.0
Inter. floor beam	1400	351	1272	16.4	1400	412	939	21.0
Arch member	1041	653	324	24.0	1254	875	332	22.8
Stiffening girder	1400	519	1099	16.0	1400	775	403	31.0
Vertical member	1400	677	316	45.7	1400	693	303	46.6
Diagonal member					609	-7	257	47.9

P: Load carrying capacity $P=20(\sigma_a - \sigma_d)/\sigma_l \tau$ ($\times 9.8$ kN),

σ_a : Allowable stress kg/cm², σ_d : Dead load stress kg/cm²,

σ_l : Live load stress kg/cm², *: Concrete allowable stress

1kg/cm²=0.098MPa

In the floor system, new stringers were added between the existing stringers to reduce the distance to 0.8 m from 1.6 m, and both new and existing stringers were supported by the continuous system. The stringers were joined to the cross beams with high strength bolts. Intermediate shoes were added to increase the load carrying capacity and to moderate the impact at the expansion joint on the span center of the end floor beam, and the intermediate floor beams were reinforced with cover plates. The RC slab, the asphalt pavement and the curb were reconstructed, and a steel deck slab was used to reduce repair time. In addition, the expansion joints were repaired, and the bridge was repainted.

Table 4 shows the effect on static load carrying capacity, P , of the additional diagonal members. Although the load carrying capacity of each member in the stiffening arch bridge was poor, the load carrying capacity of slab, stringer and stiffening girder in the reinforced bridge was substantially increased, but that of the arch member slightly decreased because the ratio of allotment of arch member to applied load was increased. As shown by the analytical calculations, these added diagonal members greatly increase the load carrying capacity of each bridge member except the arch member. Thus, it can be seen that the load carrying capacity of the reinforced bridge was increased.

3.1 Measured results

Fig.9 shows the points of measurement in the vibration test. Deflection was measured at D_i , the vibration deflection amplitude at V_i , and vibration acceleration at A_j . As a measured example, Fig.10 shows the response vibration of the bridge under a heavy moving vehicle. Using measured data of damped free vibration as shown in Fig.10(a), the natural frequencies and the corresponding vibration modes of the stiffened arch bridge were calculated, and the values for the first asymmetric mode of 3.7 Hz and the first symmetric mode of 4.3 Hz were obtained. As shown by the deflection D_4 and the deflection amplitude V_4 at $L/4$ in Fig.10(a), the large first asymmetric vibration resulted because this value of 3.7 Hz approaches the natural

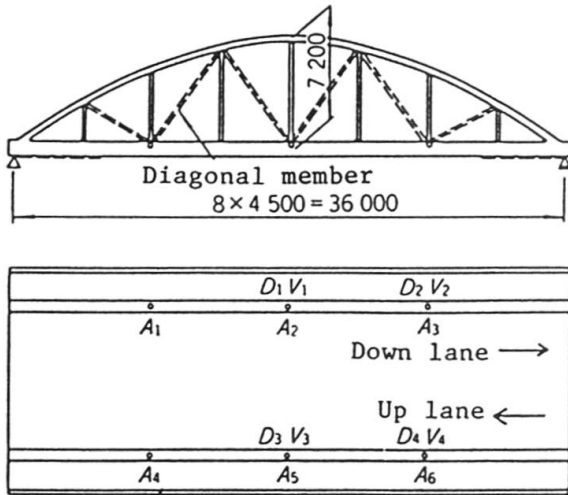


Fig.9 Measured points.

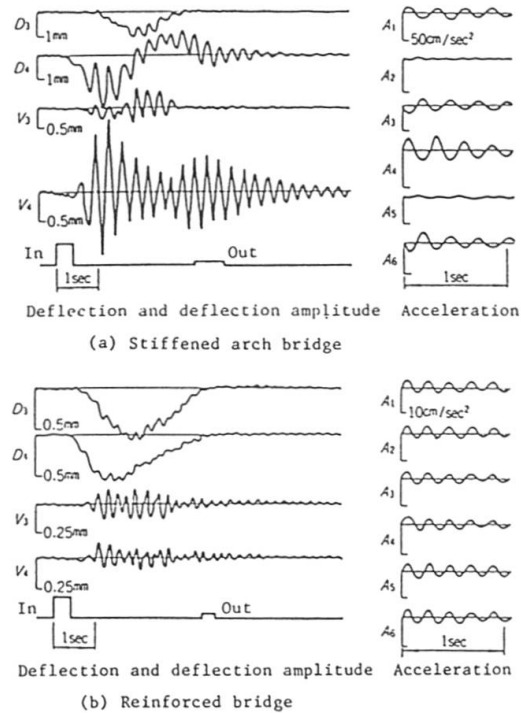


Fig.10 Response vibration.

frequency of heavy vehicles. However, response vibration in the reinforced bridge is obviously decreased at each measured point as shown in Fig.10(b), except that the acceleration at A_2 and A_5 increases slightly. In particular, as shown by the analytical study, a striking decrease of the vibration deflection at D_4 and the deflection amplitude at V_4 can be obtained by adding the diagonal members. The natural frequencies and the vibration modes of the reinforced bridge were calculated from the measured data of damped free vibration, and the values obtained were about 8 Hz for the first asymmetric mode and 4.7 Hz for the first symmetric mode. When only the first frequency was considered, the frequency increased from 3.7 Hz for the stiffened arch bridge to 4.7 Hz for the reinforced bridge, and the first vibration mode was changed, by the alteration of the bridge structure system, from asymmetric mode to symmetric mode as shown by the acceleration waves. Therefore, the resonance of the reinforced bridge with heavy vehicles can be prevented by increasing the first frequency and by changing the vibration mode. Although there may be some resonance of the 4.7 Hz frequency with that of smaller middle-sized vehicles this is not a serious problem, since the weight of such vehicles is small. Finally, it was recognized that the large first asymmetric vibration at the point $L/4$ of the reinforced bridge could be eliminated by the addition of the diagonal members.

Fig.11 shows the maximum response at each measured point under a moving dump truck. The horizontal axis in this figure is the acceleration, the vibration deflection and the deflection amplitude, and the vertical axis is the frequency. Maximum deflection and the deflection amplitude are the values of maximum double amplitude at the point where the static maximum deflection arose. The vehicle velocity in each case is also shown in Fig.11. These data are shown in more detail in Table 5. A large difference can be seen between the stiffened arch bridge and the reinforced bridge for each response value.



For example, \bar{D}_4 , \bar{A}_4 and \bar{V}_4 show that the mean value of each response value in case of a fully loaded vehicle decreases about 1/5, 1/3 and 1/4 respectively, although the vehicle velocity and the number of cases measured before and after reinforcing differ slightly. It can be seen that vibration has decreased.

Table 5 Measured result under a moving dump truck.

		Reinforcement						
		Not applied (12case)			Applied (13case)			
		Empty vehicle: E (7case) Full vehicle: F (5case)			Empty vehicle: E (6case) Full vehicle: F (7case)			
V	\bar{V}_E	=35.2 km/h, $\sigma=5.2$ km/h			\bar{V}_E =31.3 km/h, $\sigma=2.7$ km/h			
	\bar{V}_F	=42.7 km/h, $\sigma=5.9$ km/h			\bar{V}_F =32.4 km/h, $\sigma=4.4$ km/h			
Vibration deflection	D_3	E: 0.5	F: 1.2	mm	D_3	E: 0.3	F: 0.5	mm
	\bar{D}_3	0.43	1.02		\bar{D}_3	0.21	0.40	
	σ_3	0.07	0.12		σ_3	0.07	0.12	
	D_4	E: 1.0	F: 1.9		D_4	E: 0.3	F: 0.4	
	\bar{D}_4	0.67	1.58		\bar{D}_4	0.20	0.31	
	σ_4	0.17	0.18		σ_4	0.04	0.09	
Acceleration	A_4	57	47	cm/s ²	A_4	21	17	cm/s ²
	\bar{A}_4	34.9	40.0		\bar{A}_4	17.3	13.0	
	σ_4	12.6	6.2		σ_4	3.4	2.4	
	A_5	63	46		A_5	28	20	
	\bar{A}_5	29.6	25.6		\bar{A}_5	22.3	15.4	
	σ_5	15.2	10.7		σ_5	4.7	2.7	
Deflection amplitude	V_3	0.9	0.7	mm	V_3	0.5	0.5	mm
	\bar{V}_3	0.40	0.50		\bar{V}_3	0.44	0.35	
	σ_3	0.24	0.19		σ_3	0.07	0.08	
	V_4	0.4	1.3		V_4	0.3	0.3	
	\bar{V}_4	0.29	0.80		\bar{V}_4	0.28	0.19	
	σ_4	0.11	0.28		σ_4	0.04	0.04	

V: Vehicle velocity, σ : Standard deviation

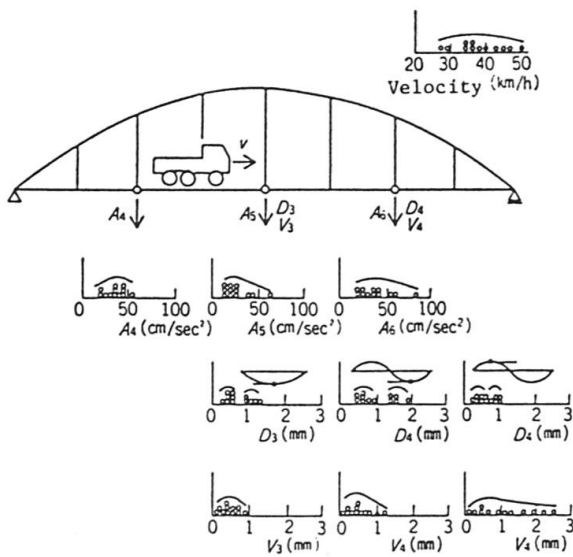


Fig.11 Maximum response values (reinforcement not applied; 12 case).

The vibration felt by the pedestrian, S , is obtained by

$$S = \left\{ \sum_{i=1}^M (\sigma_{d_i} \cdot 2\pi f_i)^2 \right\}^{1/2} \tag{15}$$

in which f_i = Frequency of vibration amplitude; σ_{d_i} = Average value of r.m.s. of deflection corresponds to f_i .

The magnitude level, VGL , of vibration is obtained by

$$VGL = 20 \log_{10} (S/S_0) \tag{16}$$

Table 6 S and VG to each structural system of bridge under a moving dump truck.

		Reinforcement															
		Not applied								Applied							
		Empty vehicle				Full vehicle				Empty vehicle				Full vehicle			
		L/2		L/4		L/2		L/4		L/2		L/4		L/2		L/4	
		V_1	V_3	V_2	V_4	V_1	V_3	V_2	V_4	V_1	V_3	V_2	V_4	V_1	V_3	V_2	V_4
1	S	0.27	0.28	0.38	0.46	0.30	0.60	0.66	0.89	0.26	0.26	0.21	0.19	0.18	0.23	0.14	0.15
	VG	0.19	0.20	0.27	0.33	0.21	0.43	0.47	0.63	0.19	0.18	0.15	0.13	0.13	0.16	0.10	0.11
2	S	0.63	0.93	0.86	1.27	0.50	0.52	0.96	0.86	0.22	0.23	0.18	0.11	0.15	0.14	0.13	0.11
	VG	0.45	0.66	0.62	0.91	0.36	0.37	0.69	0.61	0.16	0.16	0.13	0.08	0.09	0.10	0.09	0.08
3	S	0.45	0.46	0.78	0.98	0.39	0.35	0.75	0.69	0.20	0.25	0.19	0.15	0.25	0.25	0.20	0.17
	VG	0.32	0.33	0.56	0.70	0.28	0.25	0.53	0.49	0.14	0.18	0.13	0.11	0.18	0.18	0.14	0.12
4	S	0.24	0.35	0.39	0.29	0.30	0.35	0.73	0.66	0.36	0.37	0.31	0.20	0.20	0.23	0.18	0.16
	VG	0.17	0.25	0.28	0.21	0.22	0.25	0.52	0.47	0.26	0.27	0.22	0.14	0.14	0.17	0.13	0.11
5	S	0.23	0.23	0.24	0.22	0.38	0.39	0.61	1.13	0.28	0.29	0.23	0.17	0.15	0.16	0.16	0.10
	VG	0.17	0.16	0.17	0.16	0.27	0.28	0.43	0.80	0.20	0.21	0.16	0.12	0.10	0.11	0.12	0.07

Table 7 Results of field test.

Item		Reinforcement	
		Not applied	Applied
Design vehicle load		127.4 kN	196.0 kN
Slab		RC slab	Steel slab
Bridge weight		3743.6 kN	4802.0 kN
Theoretical frequency	Sym. mode	4.12 Hz	4.31 Hz
	Asym. mode	3.06 Hz	6.94 Hz
Experimental frequency	Sym. mode	4.3 Hz	4.7 Hz
	Asym. mode	3.7 Hz	about 8 Hz
Logarithmic damping coefficient		0.14 ~ 0.22 (mean 0.17)	0.09 ~ 0.11 (mean 0.10)
Theoretical deflection	at center	0.025 mm/kN	0.014 mm/kN
	at L/4	0.037 mm/kN	0.012 mm/kN
Experimental deflection	at center	\bar{D}_3 : 1.02 mm	\bar{D}_3 : 0.40 mm
	at L/4	\bar{D}_2 : 3.08 mm	\bar{D}_2 : 1.01 mm
	at L/4	\bar{D}_4 : 1.58 mm	\bar{D}_4 : 0.31 mm
Acceleration amplitude	at center	\bar{A}_5 : 25.6 cm/s ²	\bar{A}_5 : 15.4 cm/s ²
	at L/4	\bar{A}_6 : 41.2 cm/s ²	\bar{A}_6 : 14.6 cm/s ²
Deflection amplitude	at center	\bar{V}_1 : 0.82 mm	\bar{V}_1 : 0.47 mm
	at L/4	\bar{V}_4 : 1.46 mm	\bar{V}_4 : 0.19 mm
Vibration stimulus S		0.69 cm/s	0.18 cm/s
Magnitude of vibration VG		0.5	0.13



in which $S_0 = 1.4 \times 10^{-2}$ cm/s. The magnitude of vibration, VGL , of psychological effect felt by pedestrian is calculated as

$$\log_{10} VG = \begin{cases} 0.05 (VGL - 40), & VGL \leq 40 \text{ dB} \\ 0.03 (VGL - 40), & VGL > 40 \text{ dB} \end{cases} \quad (17)$$

Table 6 shows each value of S and VG based on Eqs.(15) and (17). In the stiffened arch bridge, the maximum value of S is 1.27 cm/s ($VG=0.91$). This value of 1.27 cm/s means that many pedestrians may clearly feel the vibration in walking, and that a few have difficulty walking {3}. However, the difference between the stiffening arch bridge and the reinforced bridge can be clearly seen by comparison of the values in this Table. For example, the maximum values of S and VG in the reinforced bridge become 0.37 cm/s and 0.27, a decrease of about 1/3 after reinforcing. Therefore, it can be seen that the serviceability of the bridge was improved: whereas vibration could be clearly felt before, after reinforcing it was much less noticeable.

The results of the field test are summarized in Table 7. The actual frequency was greater than the theoretical frequency. It is considered that the stiffness of the floor system affects the main structure of the reinforced bridge. In general, the actually measured static, dynamic and vibration data bore out the predictions of the theoretical calculations.

4. CONCLUSIONS

The major conclusions of this study can be summarized as follows:

- (1) The load carrying capacity of the stiffening girder was increased because the applied load was dispersed by the diagonal members.
- (2) The large first asymmetric vibration could be eliminated because the natural frequency was increased, so that the vibration mode was changed by the alteration of the bridge's structural system.
- (3) The serviceability of this bridge was improved by reducing the vibration felt by pedestrians.

Therefore, it was found by this analytical study and field test that reinforcement with diagonal members is an effective way of rehabilitating a stiffened arch bridge of this type.

REFERENCES

1. Honda, H., Y. Kajikawa and T. Kobori "Spectra of Road Surface Roughness on Bridges", J. Struct. Div., Proc. of ASCE, Vol.108, ST9/1982.
2. Kajikawa, Y. and T. Kobori "Probabilistic Approaches to the ergonomical Serviceability of Pedestrian-Bridges", Proc. of the Japan Society of Civil Engineers (JSCE), No.266/1977 (in Japanese).
3. Kobori, T. and Y. Kajikawa "Ergonomic Evaluation Methods for Bridge Vibration", Proc. of JSCE, No.230/1974 (in Japanese).
4. Kobori, T. and Y. Kajikawa "Human Response to Bridge Vibration under A Single Moving Vehicle", Proc. of JSCE, No.248/1976 (in Japanese).
5. Raghavarao, D. "Constructions and Combinational Problems in Design of Experiments", John-Wiley, 1971.
6. Seiden, E and R. Zernich "On Orthogonal Arrays", The Annals of Mathematical Statistics, May, 1965.
7. Takagi, S. et al "Report of Experimental Research on AKI-OHASHI (Nielsen System Lohse Girder Bridge)", Proc. of JSCE, No.177/1970 (in Japanese).